Lawrence Berkeley National Laboratory

Title

Dynamic Phaeodactylum tricornutum exometabolites shape surrounding bacterial communities

Permalink

https://escholarship.org/uc/item/12s164f5

Journal

New Phytologist, 239(4)

ISSN

0028-646X

Authors

Brisson, Vanessa
Swink, Courtney
Kimbrel, Jeffrey
et al.

Publication Date

2023-08-01

DOI

10.1111/nph.19051

Copyright Information

Peer reviewed

New
Phytologist

Dynamic *Phaeodactylum tricornutum* exometabolites shape surrounding bacterial communities

Vanessa Brisson[1] iD, **Courtney Swink**[1], **Jeffrey Kimbrel**[1] iD, **Xavier Mayali**[1] iD, **Ty Samo**[1] iD,
Suzanne M. Kosina[2] iD, **Michael Thelen**[1] iD, **Trent R. Northen**[2,3] iD and **Rhona K. Stuart**[1] iD

[1]Physical and Life Sciences Directorate, Lawrence Livermore National Laboratory, Livermore, CA 94550, USA; [2]Environmental Genomics and Systems Biology Division, Lawrence Berkeley

National Laboratory, Berkeley, CA 94720, USA; [3]The DOE Joint Genome Institute, Lawrence Berkeley National Laboratory, Berkeley, CA 94720, USA

Author for correspondence:
Vanessa Brisson
Email: brisson2@llnl.gov

Summary

- Roles of different ecological classes of algal exometabolites in regulating microbial community composition are not well understood. Here, we identify exometabolites from the model diatom *Phaeodactylum tricornutum* and demonstrate their potential to influence bacterial abundances.
- We profiled exometabolites across a time course of axenic algal growth using liquid chromatography–tandem mass spectrometry. We then investigated growth of 12 bacterial isolates on individual-identified exometabolites. Lastly, we compared responses of a *P. tricornutum*-adapted enrichment community to additions of two contrasting metabolites: selective growth substrate 4-hydroxybenzoic acid and putative signaling/facilitator molecule lumichrome.
- We identified 50 *P. tricornutum* metabolites and found distinct temporal accumulation patterns. Two exometabolites (of 12 tested) supported growth of distinct subsets of bacterial isolates. While algal exudates and algal presence drove similar changes in community composition compared with controls, exogenous 4-hydroxybenzoic acid addition promoted increased abundances of taxa that utilized it in isolation, and also revealed the importance of factors relating to algal presence in regulating community composition.
- This work demonstrates that secretion of selective bacterial growth substrates represents one mechanism by which algal exometabolites can influence bacterial community composition and illustrates how the algal exometabolome has the potential to modulate bacterial communities as a function of algal growth.

Introduction

Microalgae play important roles in global carbon cycling and industrial applications for bioproduct and biofuel production (Chisti, 2007; Mata *et al.*, 2010; Falkowski, 2012). As with land plants and other host–microbial systems, microalgal activity, productivity, and stability are closely tied to surrounding microbial communities (Seymour *et al.*, 2017). However, a predictive understanding of microbial community interactions with algae is still limited (Astacio *et al.*, 2021; Deng *et al.*, 2022; Prabhakara & Kuehn, 2022).

Exometabolite release is hypothesized to be a primary way by which host organisms influence microbiome composition. Exometabolites can be broadly grouped into three ecological classes: substrate metabolites which sustain biomass production (e.g. glucose), facilitator metabolites, which enable chemical reactions (e.g. biotin (vitamin B7)), and ecological signaling molecules (e.g. *N*-acetyl homoserine lactone; Moran *et al.*, 2022). Since algae are the predominant primary producers in many aquatic ecosystems, the most direct hypothesized mechanism of influence

is through release of specialized substrate metabolites. In algal bloom communities, microbial succession is controlled by substrate utilization (Teeling *et al.*, 2012), certain taxa in these blooms specialize to specific substrate types (Orellana *et al.*, 2022), and exudates from different algae support distinct functional microbial communities (Kieft *et al.*, 2021). In model algal–bacterial co-cultures with the diatom *Thalassiosira pseudonona*, characterization of exometabolite uptake showed specialization between bacterial partners (Ferrer-Gonzalez *et al.*, 2021). Along with selective substrate utilization, there are examples of algal exometabolites with multifaceted effects: the exometabolites rosmarinic and azelaic acids from the diatom *Asterionellopsis glacialis* can influence bacterial motility and possibly quorum sensing (Shibl *et al.*, 2020), placing them in both the substrate and ecological signaling categories. Additionally, *p*-coumarate, a metabolite released during *Emiliana huxleyi* senescence, has been linked to a shift from mutualistic to algicidal activity of the bacterium *Phaeobacter inhibens* (Seyedsayamdost *et al.*, 2014). In a community context, microbial abundances have been shown to change in response to metabolite composition in simplified

systems with defined suites of metabolites (Fu *et al.*, 2020). Previous work has shown that different algae have distinct exometabolomes (Brisson *et al.*, 2021), but the dynamics of release, and physiological function of these exometabolites are unknown, as are their respective effects on surrounding microbial communities. Given these impacts of exometabolites on algal–bacterial interactions, characterization of algal exometabolomes and their roles is critical for understanding these systems.

Direct analysis of the spent media, targeting metabolites that are specific to that fraction relative to the endometabolome, is needed to further understand algal–bacterial interactions. Intracellular metabolites have been used as a proxy for exometabolites (Thornton, 2014; Seymour *et al.*, 2017). Used in conjunction with transcriptomics, this approach has produced insights into algal–bacterial interactions and metabolite exchange dynamics (Uchimiya *et al.*, 2021). However, recent work with several algal strains suggests that the algal exometabolome composition differs significantly from the endometabolome (Brisson *et al.*, 2021). Algal exometabolomics, particularly for saltwater algae, presents technical challenges due to high salts and low metabolite concentrations (Ferrer-Gonzalez *et al.*, 2021), but recent studies have started to address this knowledge gap. The exometabolomes of the eukaryotic microalgae *Asterionellopsis glacialis*, *Thalassiosira pseudonona*, *Thalassiosira rotula*, *Phaeodactylum tricornutum*, *Microchloropsis salina*, *Chlamydomonas reinhardtii*, and *Desmodesmus intermedius* have been characterized using untargeted and targeted metabolomic approaches (Becker *et al.*, 2014; Shibl *et al.*, 2020; Brisson *et al.*, 2021; Ferrer-Gonzalez *et al.*, 2021). As exometabolite characterization expands, the next challenge is to integrate that knowledge with the effects of individual bacterial strain responses to understand interactions in a complex microbiome.

In this study, we investigate the role of exometabolites from the model diatom *Phaeodactylum tricornutum* in shaping surrounding microbial communities. We set out to test the hypothesis that algal exudates drive microbial community composition and to identify specific algal exometabolites that can be linked to specific changes in algal-associated microbial communities. To get a baseline understanding of microbial community responses before investigating and manipulating individual metabolites, we used 16S amplicon sequencing analysis to investigate community composition responses to algal exudates and algal presence. We then conducted a time-resolved metabolomic analysis to characterize exudates from axenic *P. tricornutum* and identify specific exometabolites (defined here as metabolites primarily detected in the spent media relative to the cell pellet). We next conducted growth assays on a subset of identified exometabolites with bacterial isolates obtained from *P. tricornutum*-associated communities to identify exometabolites from the 'substrate' ecological class. Based on results from these assays, we chose one substrate exometabolite and one contrasting signaling or facilitator exometabolite to further examine the response of microbial community composition to these exometabolites. Together, this allowed us to investigate the interacting roles of exometabolites, algae, and bacteria, and to identify a mechanism by which substrate algal exometabolites can influence community structure in a predictable manner.

Materials and Methods

Organisms

We used the model diatom *Phaeodactylum tricornutum* Bohlin strain CCMP 2561, 10 phycosphere bacterial isolates from *P. tricornutum* phycosphere enrichment cultures, and two non-phycosphere bacterial isolates from seawater. Bacterial isolate origins and identifications are summarized in Table 1. All bacterial isolates were isolated in our laboratory and have been described elsewhere (Chorazyczewski *et al.*, 2021; Mayali *et al.*, 2022). Enrichment cultures were from the same phycosphere enrichments used to obtain the bacterial isolates and have been described elsewhere (Samo *et al.*, 2018; Kimbrel *et al.*, 2019).

Growth medium

Experiments were conducted using Enriched Saltwater Artificial Water (ESAW) with F/2 medium trace metals and vitamins, which has been described previously (Guillard & Ryther, 1962; Harrison *et al.*, 1980; Berges *et al.*, 2001; Brisson *et al.*, 2021). The medium contained salts, phosphate, trace metals, and vitamins as described in Supporting Information Methods S1. For bacterial isolate growth experiments, levels of nitrogen and phosphorus were in excess compared with carbon, and nitrogen was provided as equimolar concentrations of nitrate and ammonium, since not all bacteria can assimilate nitrate. For all other experiments, nitrogen was provided as nitrate.

Microbial community response to algae and algal exudates

In the first experiment (Fig. S1a), microbial community response to three algal conditions was tested (five replicates of each condition): algae present, algal spent medium, and algal-free control. Before the experiment, 125 ml glass Erlenmeyer flasks were baked at 500°C for 2 h to remove residual organic matter. For the algae-present condition, five flasks were prepared with ESAW medium (50 ml) and inoculated with 2 ml of 1-wk-old *P. tricornutum* culture. For the algal spent medium condition, five flasks were prepared with spent medium from a 1-wk-old *P. tricornutum* culture that was filtered through a 0.2 μm filter to remove algal cells. Preliminary experiments indicated that *P. tricornutum* completely depletes nitrate and phosphate in the medium (Fig. S2), so phosphate and nitrate were replenished in algal spent medium to original ESAW concentrations by adding 0.005 g l^{-1} NaH$_2$PO$_4$·H$_2$O and 0.075 g l^{-1} NaNO$_3$ from 1000× stock solutions before inoculation with bacteria. These additions did not change the pH of the spent medium (Fig. S3). Five algal-free control flasks were prepared with ESAW medium without addition of algae, algal spent medium, or other carbon sources beyond what was present in the base medium.

To obtain starting bacterial inoculum, two previously described phycosphere enrichment cultures (bacterial communities enriched to grow in close association with algae) were combined (Samo *et al.*, 2018; Kimbrel *et al.*, 2019). Enrichments were grown separately in ESAW medium for 1 wk. Cultures were

Table 1 Bacterial isolates and corresponding microbial community ASVs with exact matches to the 16S-V4 region.

Isolate origin[1]	Taxonomic group (phylum or proteobacterial class)	Bacterial isolate	IMG genome ID	Exact match 16S-V4 ASV	ASV mean relative abundance under different growth conditions		
					Algal-free control (%)	*Phaeodactylum tricornutum* spent medium (%)	*Phaeodactylum tricornutum* present (%)
Phycosphere enrichments	Alphaproteobacteria	*Oceanicaulis 13A*	2744055042	ASV12	0.25	4.29	8.06
	Alphaproteobacteria	*Roseibium 13C1*	2754412429	ASV6	3.36	6.75	2.53
	Alphaproteobacteria	*Thalassospira 13M1*	2744054425	ASV23	0.06	0.50	0.01
	Alphaproteobacteria	*Yoonia 4BL*	2751186040	–	–	–	–
	Bacteroidota	*Arenibacter ARW7G5Y1*	2744054426	ASV34	< 0.01	0.52	0.02
	Bacteroidota	*Algoriphagus ARW1R1*	2747842515	ASV9	0.12	8.40	7.72
	Alphaproteobacteria	*Stappia ARW1T*	2758568492	–	–	–	–
	Alphaproteobacteria	*Devosia EAB7W2*	2757320511	ASV18	0.01	2.53	0.19
	Gammaproteobacteria	*Alcanivorax EA2*	2778261710	ASV14	11.70	0.03	0.09
	Gammaproteobacteria	*Marinobacter 3-2*	2785510723	ASV1	29.16	33.03	12.21
Seawater	Alphaproteobacteria	*Amylibacter N2S*	2838011328	–	–	–	–
	Alphaproteobacteria	*Sulfitobacter N5S*	2834034572	–	–	–	–
Total					44.66	56.05	30.83

[1]Isolate origin and identification are from Mayali *et al.* (2022) ASV, amplicons sequence variants; IMG, Integrated Microbial Genomes database.

filtered (0.8 µm pore size, 45 mm diameter Supor membrane filter (Pall Corp., Port Washington, NY, USA)) to remove algal cells but allow bacterial cells to pass through. Filtrates were used to inoculate all 15 flasks with 2 ml (1 ml from each enrichment).

All flasks were incubated with shaking (90 rpm, 22°C; 12 h : 12 h, light : dark; 3500 lux illumination). Algal growth was monitored by measuring chlorophyll *a* fluorescence using a Trilogy Fluorometer (Turner Designs, San Jose, CA, USA) with the Chlorophyll *In-Vivo* Module.

Flasks were maintained as fed batch/semi batch systems, with sample collection and partial medium replacement at 6, 8, and 10 d of incubation. This timing was selected based on the time for *P. tricornutum* to reach stationary phase based on previous work with this organism (Brisson *et al.*, 2021). On sample collection days, 25 ml samples were collected from each flask, and flasks were replenished with 25 ml of the appropriate fresh or algal spent medium for that flask's condition. One ml from each sample collected was fixed for flow cytometry by adding 100 µl 37% formaldehyde. However, the flow cytometry samples were lost due to instrumentation problems. The remaining 24 ml sample was filtered onto a 45 mm diameter, 0.2 µm pore size Supor membrane filter (Pall Corp.). Filters were frozen at −80°C until DNA extraction. DNA extractions were conducted as described in Methods S2.

Sequencing was performed through Laragen Inc. (Culver City, CA, USA), using the earth microbiome project protocol. The 515F (GTGYCAGCMGCCGCGGTAA; Parada *et al.*, 2016) and 806R (GGACTACNVGGGTWTCTAAT; Apprill *et al.*, 2015) primers were used to amplify and sequence the 16S-V4 region. Sequencing was performed on an Illumina MiSeq (Illumina, San Diego, CA, USA) using the MiSeq v.2 PE150 Reagent Kit. Sequencing reads were processed using the DADA2 package

(v.1.20.0) to generate an amplicon sequence variant (ASV) table (Callahan *et al.*, 2016), as detailed in Methods S3 (also Fig. S4).

Algal exometabolomics

Our second experiment (Fig. S1b) was conducted in 20 replicate flasks. Flasks were baked to remove residual organic matter (500°C for 2 h), filled with ESAW medium (50 ml each), inoculated (2 ml each) from a 1-wk-old axenic *P. tricornutum* culture, and incubated as described above for the community response experiment. At each metabolite collection time point (0, 3, 6, 9, and 12 d; Fig. S5), four flasks were destructively sampled for metabolomics analysis of spent medium and cell pellets as described previously (Brisson *et al.*, 2021). Briefly, cell pellets were collected by centrifugation at 5000 *g* and 4°C for 8 min. The supernatant was filtered through a 0.45 µm pore size filter (which removed *P. tricornutum* cells) and frozen at −80°C. Cell pellets were resuspended in 1 ml 0.2 µm filtered sterile water, frozen at −80°C, and lyophilized. Lyophilized cells were disrupted by vortexing with a steel ball three times for 5 s each, resuspended in 50 ml 0.2 µm filtered sterile water, filtered through a 0.45 µm pore size filter, and frozen at −80°C.

Solid phase extraction (SPE) was used to extract metabolites from all samples for analysis. Samples (filtered spent medium and filtered water extracts of disrupted cell pellets) were thawed, and 30 ml of each sample was acidified by adding 300 µl of 1 M HCl. Bond Elut PPL columns (Agilent, Santa Clara, CA, USA) were rinsed with 3 ml HPLC grade methanol followed by 6 ml ultrapure water. Acidified samples were passed through prepared columns. Columns were rinsed with 3 ml of 0.01 M HCl and allowed to air dry for 5 min. Metabolites were eluted with 1 ml HPLC grade methanol, dried in a vacuum centrifuge, and

resuspended and prepared for analysis as previously described (Zhalnina *et al.*, 2018; Brisson *et al.*, 2021; Swift *et al.*, 2021). Briefly, extracts were dried in a vacuum centrifuge, resuspended in 150 µl methanol containing ^{13}C and ^{15}N labeled matrix control standards, filtered through a 0.2 µm pore size filter, and transferred to an autosampler vial for analysis. Although we did not measure recovery, a previous study found that PPL columns recovered *c.* 60% of dissolved organic carbon from marine samples (Green *et al.*, 2014).

Metabolomes were analyzed with liquid chromatography–tandem mass spectrometry (LC–MS/MS). LC–MS/MS instrumentation and parameters are detailed in Table S1. Metabolite identifications were obtained using Metabolite Atlas (https://github.com/biorack/metatlas) to identify features with *m/z*, retention time, and fragmentation spectra matched to a library of analytical standards run in our laboratory under the same LC–MS/MS analysis conditions (Bowen & Northen, 2010; Yao *et al.*, 2015).

Bacterial isolate growth assays

In our third experiment (Fig. S1c), 12 selected metabolites were tested for their ability to support growth as the primary carbon source for each of the bacterial isolates. For each metabolite, ESAW medium was prepared with the added metabolite at a total carbon concentration of 60 ppm. This concentration was chosen as *c.* 10 times the previously observed DOC concentration in *P. tricornutum* spent medium (Brisson *et al.*, 2021) in order to stimulate sufficient growth for detection. Each metabolite was tested with each bacterial isolate in triplicate wells with replicate positions randomized across the 96-well flat-bottom plates. Negative controls (no added metabolite) were also included. Plates were incubated with shaking (90 rpm, 24°C). OD_{600} was measured daily for 8 d using a Cytation5 plate reader (BioTek, Winooski, VT, USA).

Microbial community response to selected exometabolites

For our final experiment (Fig. S1d), two of the identified exometabolites (4-hydroxybenzoic acid and lumichrome) were selected to examine their influence on bacterial community composition. For this experiment, five replicate flasks of each of the same three algal conditions described above (algae present, spent media, and algae-free control) were prepared with the addition of 0.01 mM of the metabolite being tested (5 replicates × 3 algal conditions × 2 metabolite conditions (4-hydroxybenzoic acid, lumichrome) = 30 total flasks). These were run concurrently with the no-metabolite conditions described above (Fig. S1a), which served as the control conditions. The concentration of 0.01 mM was selected so that the added metabolite did not overwhelm algal metabolites present in the algal spent medium and algae-present conditions, and because previous work with lumichrome indicated that this concentration impacted *P. tricornutum* growth (Brisson *et al.*, 2021). This concentration corresponds to the addition 1.4 ppm and 0.8 ppm total organic carbon for lumichrome and 4-hydroxybenzoic acid, respectively. For

comparison, our previous work found that the organic carbon content of *P. tricornutum* spent medium after 8 d of growth (comparable to the spent medium used in this study) was 8 ± 2 ppm (Brisson *et al.*, 2021). Thus, metabolite additions corresponded to an organic carbon increase of 10% to 20%. Bacterial inoculum was added, flasks incubated, samples collected, DNA extracted, and sequenced, and sequences analyzed as described above for the microbial community response to algae section. When growth medium was exchanged (days 6, 8, and 10 as described above), replenishment medium was supplemented with 0.01 mM of the appropriate metabolite for each flask.

Algal growth assays

To investigate the impacts of exogenous metabolite additions on algal growth, axenic *P. tricornutum* was grown under three different media conditions: ESAW with 0.01 mM 4-hydroxybenzoic acid, ESAW with 0.01 mM lumichrome, and ESAW without metabolite additions. Three replicate flasks (125 ml) were prepared with medium (50 ml) and inoculated with 2 ml of 1-wk-old *P. tricornutum* culture. Flasks were incubated as described above for the community response experiment. One ml samples were collected from each flask at 0, 2, 4, 6, 8, and 9 d after inoculation, and chlorophyll *a* fluorescence was measured using a Trilogy Fluorometer (Turner Designs) with the Chlorophyll *In-Vivo* Module.

Statistical analyses

The 16S microbial community data were analyzed in R using the PHYLOSEQ (v.1.40.0), VEGAN (v.2.6-2), and ANCOM-BC (analysis of compositions of microbiomes with bias correction, v.1.6.4) packages (McMurdie & Holmes, 2013; Lin & Das Peddada, 2020). Because ASV relative abundance data are inherently compositional (Gloor *et al.*, 2017), ANCOM-BC, which uses log ratios analogous to Aitchison's method (Aitchison, 1982; Lin & Das Peddada, 2020), was used to adjust for compositionality before all downstream analyses. Further analyses of microbial community, metabolomics, and bacterial and algal growth were conducted in PYTHON using the PANDAS (v.1.1.5) and SCIPY (v.1.5.2) packages. Details of statistical analyses are in Methods S4, and analysis scripts are available on GitHub (https://github.com/vbrisson/Algal_Exometabolites_Shape_Bacterial_Communities).

Results

Phaeodactylum tricornutum exudates and algal presence drive microbial community composition

In the first experiment (Fig. S1a), we investigated the impacts of algal presence and algal exudates on a microbial community that had previously been enriched to grow with algae (Samo *et al.*, 2018; Kimbrel *et al.*, 2019). 16S amplicon community analysis revealed this to be a relatively simplified bacterial community. After removing mitochondrial and chloroplast sequences

(30 sequences) and low prevalence ASVs (644 ASVs, see Methods S3 for prevalence criteria), there were 64 bacterial ASVs and no archaeal ASVs (Figs S6, S7). All 64 ASVs could be identified at the family level, and 60 could be identified at the genus level, representing 42 genera. Half of the ASVs were low abundance (< 0.1% mean relative abundance), while five were high abundance ASVs (> 5% mean relative abundance).

Microbial communities grown with algal spent medium from late log (day 7) or with algae present were distinct from algal-free controls (no added organic carbon beyond base ESAW medium and any carryover with bacterial inoculum) and from each other based on both the principal coordinate analysis (PCoA) and a permutational analysis of variance (PERMANOVA). Communities grown with algal spent medium were intermediate between those grown with algae present and algal-free controls along the first principal coordinate axis, which explained 56.4% of the variance (Fig. 1). The second principal coordinate axis further differentiated communities grown on algal spent medium from the other conditions and differentiated between time points within each condition. Algal condition (algae present, algal spent medium, or control), time, and their interaction were all significant drivers of microbial community composition (PERMANOVA, Table S2). Community alpha diversity, as measured by Shannon Diversity Index, was driven by algal presence, and also increased over time (Table S3; Fig. S8).

Algal presence and spent medium shifted relative abundances of most ASVs in the same direction compared with controls (Fig. 2). Of the 32 ASVs with mean relative abundance of at least 0.1%, 28 were significantly differentially abundant between algal spent medium and controls, and a distinct set of 30 were differentially abundant between algae present and controls (Figs 2a,

S7, S9) based on a differential abundance analysis conducted with ANCOM-BC with correction for multiple comparisons. Only six ASVs had divergent responses to algal presence and spent medium. These included four (*Marinobacter* ASV3, *Roseibium* (*Labrenzia*) ASV6, *Thalassospira* ASV7, and *Thalassospira* ASV23) which increased with spent medium but decreased with algae, and two (*Roseitalea* ASV 29 and *Maricaulis* ASV32) which decreased with spent medium but increased with algae. In general, members of the Baceroidota phylum increased in relative abundance in response to both algal presence and spent medium, while Gammaproteobacteria decreased in relative abundance, and responses of Alphaproteobacteria were mixed. Chi-squared test indicated that these phylogenetic effects were statistically significant ($P < 0.001$), while linear least-squares regression analysis indicated that there was a significant correlation ($P < 0.001$, Pearson's $R^2 = 0.52$) between the responses (log fold changes compared with control) of ASVs to algal spent medium and to algal presence (Fig. 2b).

Phaeodactylum tricornutum produces diverse exometabolites

By profiling spent media and cell pellets from *P. tricornutum*, we identified 50 metabolites recoverable by SPE, including organic acids, vitamins, amino acids, and nucleosides/nucleobases, as well as derivatives of these (Fig. 3; Tables S4, S5). The majority of identified metabolites (43 out of 50) were nitrogen containing compounds. To better distinguish exometabolites resulting of excretion or secretion from metabolites originating from lysed cells, we compared spent media and cell pellet metabolomes, since cell lysis products were likely to have higher abundance in the cell pellet fraction. Metabolite profiles from cell pellets and spent medium were distinct from each other, and most individual metabolites were highly associated with one or the other sample type (Fig. 3a). Hierarchical clustering based on abundance patterns across samples grouped metabolites into two main clusters: those primarily associated with the spent media (26 metabolites) and those primarily associated with the cell pellets (24 metabolites). We thus define exometabolites based on that clustering as those primarily associated with spent medium (Fig. 3a). As a compound class, organic acids were more highly associated with the exometabolome (chi-squared test P-value = 0.002). Although we observed trends of higher associations of nucleosides/nucleobases and amino acids with cell pellets and higher association of vitamins with spent medium, these associations were not statistically significant. Three indole-containing metabolites (indole3-acetic acid, indole-3-pyruvic acid, and 5-hydroxyindoleacetic acid) and the additional plant hormone salicylic acid all clustered as exometabolites.

Exometabolite production was dynamic, with different exometabolites accumulating in the spent medium during different algal growth phases (Fig. 3b). For example, two exometabolites (galacturonic acid and pyridoxine) only accumulated during late log and stationary phases but were not detected earlier in growth. At the other extreme, 5′-methylthioadenosine accumulated through log phase but did not continue to accumulate in stationary phase.
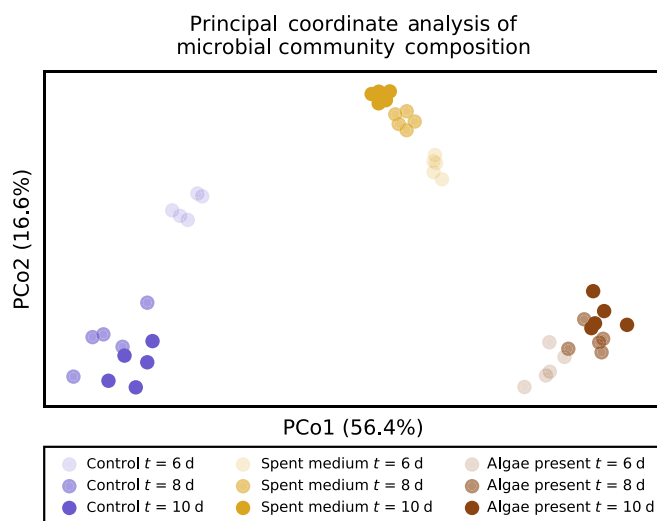
Principal coordinate analysis of microbial community composition

Fig. 1 Principal coordinate analysis (PCoA) showing differences in microbial community composition using Jensen–Shannon Divergence between samples. Each point represents one biological replicate sample (flask × time point). All replicates for each condition and time point are shown. Colors represent different growth conditions of algae (*Phaeodactylum ricornutum*) present (brown), algal spent medium (yellow), or algal-free control (blue). Shading indicates the time of sample collection at 6 d (light), 8 d (medium), or 10 d (dark).
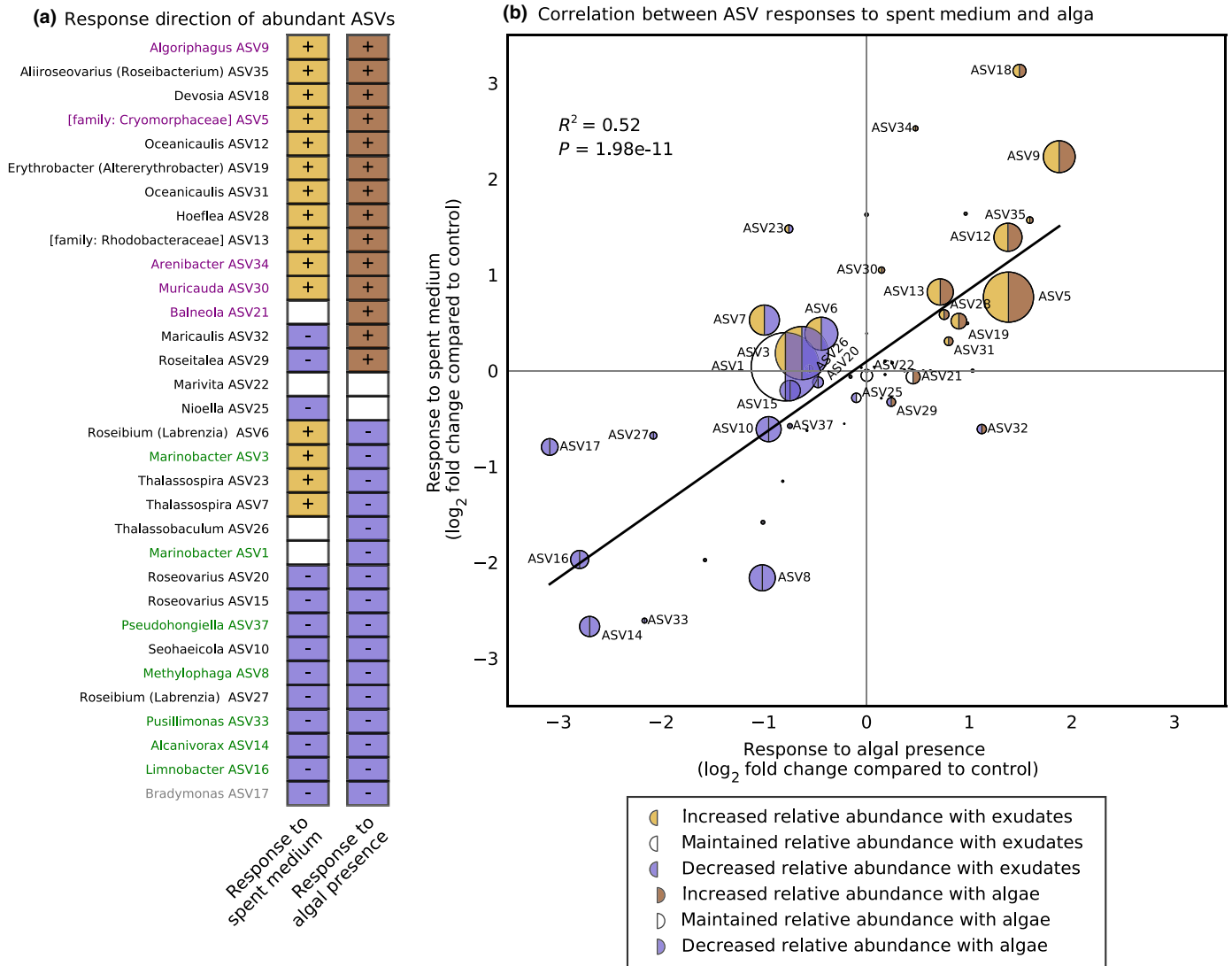
Fig. 2 Response of individual amplicon sequence variants (ASVs) to algal (*Phaeodactylum ricornutum*) presence and algal spent medium compared with algal-free controls. (a) Direction of ASV responses to algal presence and algal spent medium. Only the ASVs with at least 0.1% mean relative abundance are included. ASVs are ordered by response to algal presence. ASV label colors indicate taxonomic groups (purple, Bacteroidota; green, Gammaproteobacteria; black, Alphaproteobacteria; gray, other). Colors and symbols in boxes indicate statistically significant differences in relative abundance compared with algae-free controls based on differential abundance testing with analysis of compositions of microbiomes with bias correction (ANCOM-BC), which corrects of data compositionality (15 samples per algal condition). Differences were considered statistically significant if the Benjamini/Hochberg adjusted *P*-value from the differential abundance analysis was < 0.05. '+' indicates a significant increase in relative abundance compared with control, and '−' indicates a significant decrease compared with control. (b) Correlation between ASV responses to spent medium and algal presence. Each circle represents one ASV. Circle size is proportional to mean relative abundance across all 45 samples (15 flasks × 3 time points). Shading indicates statistically significant responses to algal presence (left side of circle) and algal spent medium (right side of circle) using the same significance criteria as in part (a). The diagonal line shows the linear fit to the data, with Pearson's R^2 and *P*-values indicated in the upper left of the plot. All 64 ASVs are included in this plot, but only ASVs with at least 0.1% mean relative abundance are labeled.

Individual exometabolites impact bacterial isolate growth

The above results established effects of algal exometabolites in general (spent medium) on microbial community composition (Fig. S1a, first experiment) and identified exometabolites produced by *P. tricornutum* (Fig. S1b, second experiment). To establish connections between individual metabolites and bacteria, we conducted a third experiment with a select set of 12 bacterial isolates (Fig. S1c). The isolates were representative of ASVs detected

in the microbial community response experiment. Of the 10 bacterial isolates originating from phycosphere enrichments, eight had 100% sequence identity between their 16S sequence and an ASV (Table 1). Together these exact match ASVs represented between 44.7%, 56.0%, and 30.8% total relative abundance under the algal-free, spent medium, and alga present growth conditions, respectively.

Based on accumulation in the exometabolome, 12 metabolites were selected to test as growth substrates. Six metabolites were
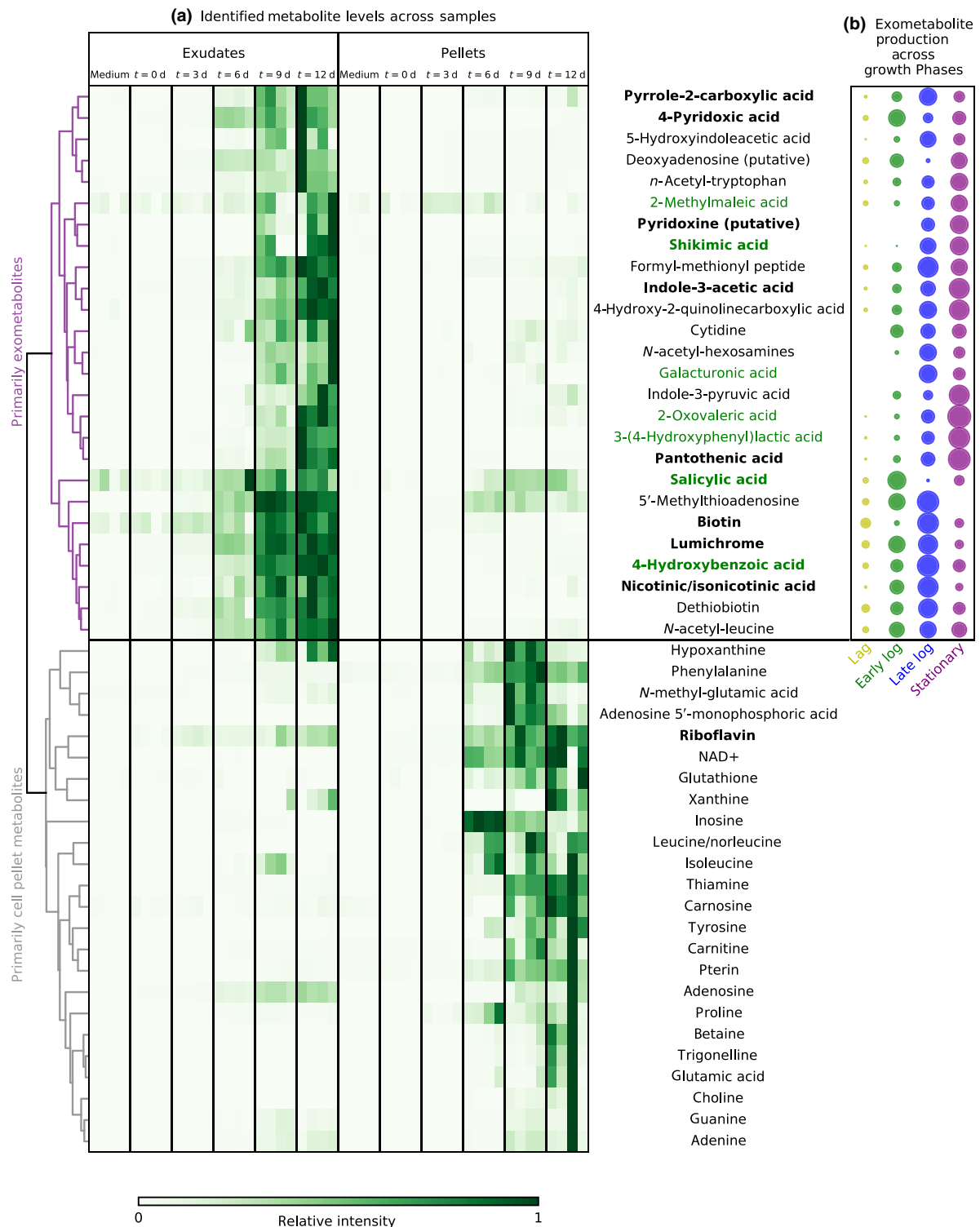
Fig. 3 *Phaeodactylum tricornutum* metabolite production across growth phases. (a) Heatmap showing 50 identified metabolites' relative intensities across samples. Each column represents one replicate flask, and samples are grouped by sample type and time point as indicated above the plot. Each row represents one metabolite (or indistinguishable isomers). Heatmap coloring at each point corresponds to the relative intensity for each metabolite in each sample. Relative intensity is the signal intensity for a given metabolite in a sample divided by the maximum signal intensity observed for that metabolite (scale of 0–1). Thus, relative intensities can be compared across samples, but not between metabolites. (b) Exometabolite accumulation in the spent medium during each growth phase. Circle size represents the production (relative intensity increase) during each growth phase, calculated as the difference between the mean signal intensities (means of four spent medium replicates) for the two sampling time points bracketing that growth phase. Circle colors indicate different growth phases: yellow, lag phase; green; early log phase; blue, late log phase; purple, stationary phase, and correspond to colors in Supporting Information Fig. S5. Metabolites are ordered based on hierarchical clustering, as indicated by the dendrogram to the left of the heatmap. Metabolite name colors indicate nitrogen content (black, contains nitrogen; green, does not contain nitrogen). Metabolite names in bold were used in the bacterial isolate growth experiment.

selected from each of two contrasting groups: organic acids (Fig. 4, bottom six), which were expected to be potential growth substrates, and vitamins/vitamin derivatives (Fig. 4, top six), which were expected to have other indirect impacts (facilitator or signaling functions). While we did not expect growth on the facilitator or signaling molecules, there are some examples of bacterial growth with plant hormones such as indole-3-acetic acid (Leveau & Gerards, 2008; Laird et al., 2020), and vitamins such as vitamin B3 (nicotinic acid/nicotinamide; Hu et al., 2019), as carbon sources. We chose to include riboflavin despite its clustering with the cell pellet metabolites because we had chosen the exometabolite lumichrome, which is a degradation product of riboflavin.

A subset of exometabolites supported growth of specific bacterial isolates as the primary source of organic carbon (ESAW medium contains a small amount of organic carbon in vitamins and EDTA as described in Methods S1). Growth was detected as a statistically significant increase (P-value < 0.05, t-test with correction for multiple comparisons, three replicates) in optical density compared with no-metabolite added controls. Of the 12 metabolites tested, two supported growth of at least one of the 12 bacterial isolates (Figs 4, S10). Both growth supporting metabolites were organic acids and not vitamins or their derivatives. 4-

Hydroxybenzoic acid was the most widely utilized substrate under the conditions tested and supported the growth of four isolates, while shikimic acid supported the growth of two isolates.

To relate responses to 4-hydroxybenzoic acid and shikimic acid to genetic potential, we searched the previously sequenced genomes of these isolates (Mayali et al., 2022) for genes for four enzymes related to 4-hydroxybenzoic acid degradation: 4-hydroxybenzoate 3-monooxygenase (gene: pobA), 4-hydroxybenzoate decarboxylase (genes: bsdC, bsdD), 4-hydroxybenzoate polyprenyltransferase (gene: ubiA), and 4-hydroxybenzoate-CoA ligase (genes: hbaA, hcl). We also searched for genes for three enzymes related to shikimate degradation: quinate dehydrogenase (genes: quiA), shikimate dehydrogenase (genes: qsuD), and dehydroshikimate dehydratase (genes: quiC, qsuB). KEGG searches were conducted with KOFAMSCAN v.1.3.0 with the KEGG v.98 database, and PATRIC terms were searched for using patricbrc.org (see Table S6 for search details and Table S7 for results). Of the 4-hydroxybenzoic acid degradation genes, only pobA and ubiA were identified in the isolate genomes. All isolate genomes except for Algoriphagus ARW1R1 and Arenibacter ARW7G5Y1 contained ubiA, while pobA was found in three of the four isolates which grew on 4-hydroxybenzoic acid (Thalassospira 13 M1, Roseibium 13C1, and Stappia ARW1T) and three other isolates which did not grow on 4-hydroxybenzoic acid. Of the shikimic acid degradation genes, quiA was identified in one isolate that grew on shikimate (Alcanivorax EA2), while qsuD was identified in three isolates, including the other isolate that grew on shikimate (Stappia ARW1T). None of the isolate genomes contained quiC/qsuB.

Specific exometabolites influence relative abundance of bacteria in a complex community

For our fourth experiment (Fig. 1d), we selected two algal exometabolites, 4-hydroxybenzoic acid and lumichrome, to test whether exometabolites can generate similar bacterial responses in a community as observed in isolate cultivation (i.e. increase abundance). 4-Hydroxybenzoic acid was chosen because it selectively supported growth of specific bacterial isolates in the experiment above. Lumichrome was selected as a contrasting exometabolite: a representative vitamin derivative and potential facilitator or signaling molecule, with the potential to impact microbial community composition indirectly, potentially through impacts on algal growth (Brisson et al., 2021). Additionally, both exometabolites had similar accumulation profiles, with maximum accumulation during log phase growth (Fig. 3b). Because the two microbial community experiments (Fig. S1a,d) were conducted, sequenced, and analyzed together, this analysis contains the same 64 ASVs described above (Fig. S7).

Exogenous metabolite additions had significant impacts on bacterial community compositions, both with and without P. tricornutum present, based on PCoA and PERMANOVA. As with the communities without metabolite addition, the first principal coordinate of the PCoA, which accounted for 30.9% of the variance, separated samples primarily by algal treatment (algae present, algal spent medium, and control), with algal spent medium
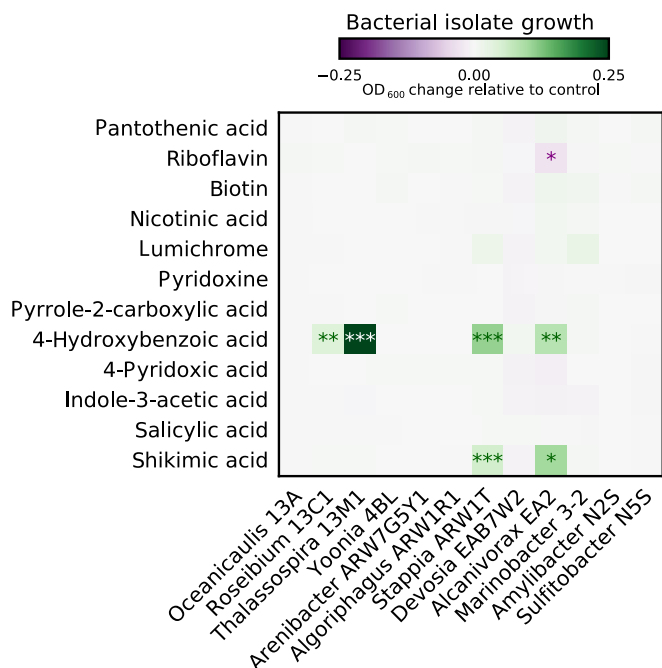

Fig. 4 Growth of algal-associated bacterial isolates on select algal (*Phaeodactylum ricornutum*) exometabolites. Heatmap color intensity corresponds to the mean increase (green) or decrease (purple) in final optical density for each isolate and metabolite combination compared with control for that isolate with no added metabolite. Means are for three biological replicates. Statistically significant differences compared with control with no added metabolite are indicated based on P-values from Student's t-tests and corrected for multiple comparisons using the Benjamini/Hochberg method. Significance codes for adjusted P-values: ***, P < 0.001; **, P < 0.01; *, P < 0.05; ·, P < 0.1. For individual data points contributing to the heatmap for the metabolites that supported growth, refer to Supporting Information Fig. S10.

being intermediate to algae present and algal-free controls (Fig. 5). The second and third principal components, accounting for 11% and 9% of the variance respectively, distinguished samples by metabolite addition, visually distinguishing the samples with added 4-hydroxybenzoic acid from those with lumichrome or no added metabolite (Fig. 5, black outlines), although this effect is less pronounced in the algal spent medium condition. PERMANOVA indicated that algal condition, metabolite addition, time, and their interactions were all significant factors affecting microbial community composition (Table S8).

4-Hydroxybenzoic acid addition drove significant changes in relative abundance of several ASVs based on a differential abundance analysis conducted with ANCOM-BC with correction for multiple comparisons (Figs 6a, S7, S11). *Thalassospira* ASVs

(ASV7 and ASV23) were the most responsive to this metabolite, with bias-corrected log fold changes of 2.4 and 1.9, respectively, in the algae-free condition, and 1.5 and 0.4, respectively, with the algae present. Notably, this included *Thalassospira* ASV23, an exact match to the 16S-V4 regions of the bacterial isolate *Thalassospira* 13M1, which exhibited the most growth (highest optical density) with 4-hydroxybenzoic acid of the 12 isolates tested (Fig. 5). *Roseibium* (*Labrenzia*) ASV6 was also responsive and matches *Roseibium* 13C1 which grew on 4-hydroxybenzoic acid. Conversely, *Alcanivorax* ASV14 responded negatively to 4-hydroxybenzoic acid addition, but isolate match *Alcanivorax* EA2 grew on 4-hydroxybenzoic acid in isolation.

Lumichrome addition also impacted relative abundances of ASVs, but the responses differed from those to 4-hydroxybenzoic
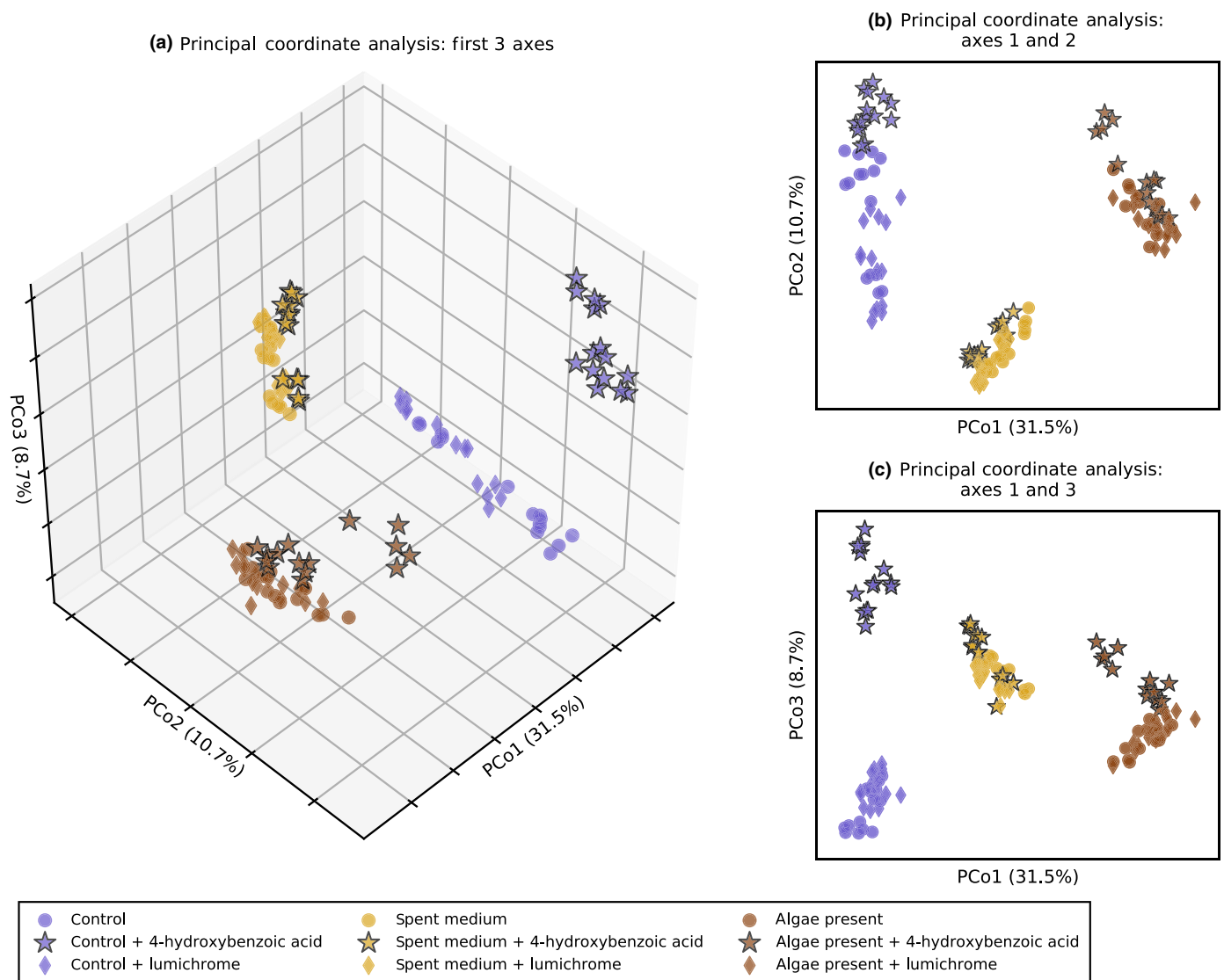

Fig. 5 Principal coordinate analysis (PCoA) showing differences in microbial community composition in response to exogenous addition of select metabolites based on Jensen–Shannon Divergence between samples. (a) Three-dimensional plot of the first three principal components. (b) Principal coordinates 1 and 2. (c) Principal coordinates 1 and 3. Each point represents one biological replicate sample (flask × time point). All replicates for each condition and time point are shown. Colors represent different base growth conditions of algae (*Phaeodactylum ricornutum*) present (brown), algal spent medium (yellow), or algal-free control (blue). Different shapes indicate different added metabolites: lumichrome (diamonds), 4-hydroxybenzoic acid (stars, black outline), and no-metabolite addition controls (circles).
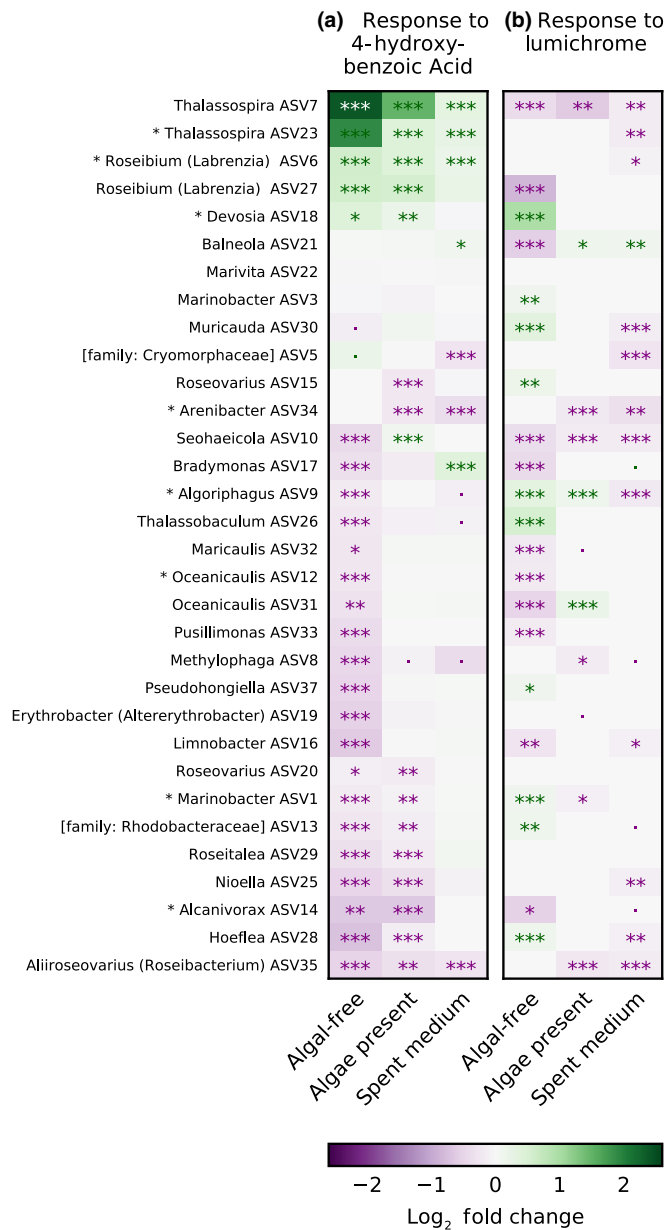
Fig. 6 Response of individual amplicon sequence variants (ASVs) to additions of exogenous metabolites compared with no-metabolite addition. (a) Response to 4-hydroxybenzoic acid. (b) Response to lumichrome. Rows represent ASVs, and ASVs with corresponding isolates are indicated with '*' before the ASV name. Columns represent base growth condition (algal-free control, algae (*Phaeodactylum ricornutum*) present, or algal spent medium). ASV order is the same in (a) and (b) to allow comparison and determined by response to 4-hydroxybenzoic acid. Heatmaps show increases (green) and decreases (purple) in relative abundance of each ASV (rows) with the addition of metabolites under each of the algal conditions (columns). Color intensity indicates log fold change compared with control (no-metabolite added) determined in the differential abundance analysis conducted with analysis of compositions of microbiomes with bias correction (ANCOM-BC), which corrects for data compositionality. This analysis was conducted with 15 samples (5 flasks × 3 time points) per algal/metabolite condition. Time points were grouped for this analysis because the effects of time, while statistically significant, were found to be much smaller than those for algal/metabolite conditions (Supporting Information Table S8). Statistically significant changes in relative abundance are indicated based on the *P*-values adjusted for multiple comparisons (Benjamini/Hochberg method) from the ANCOM-BC analysis, with significance codes for adjusted *P*-values: ***, $P < 0.001$; **, $P < 0.01$; *, $P < 0.05$; ·, $P < 0.1$. For individual comparisons and data points for each ASV under each condition with each metabolite, refer to Figs S11 and S12.

(Fig. S13). Neither 4-hydroxybenzoic acid nor lumichrome had statistically significant impacts on final chlorophyll *a* fluorescence (*P*-value = 0.56 for 4-hydroxybenzoic acid and 0.06 for lumichrome based on Student's *t*-test) in this experiment.

Discussion

Our findings support the hypothesis that algal exudates can significantly influence microbial community composition, but also indicate the importance of other factors that arise with algal presence. The microbial communities grown on algal exudates were intermediate and closer to the algae-present communities, indicating that algal exudates shifted communities toward the algae-present composition (Fig. 1). These results align with a previous study using porous microplates, which exclude the effects of attachment but include algal presence, which identified four bacterial genera (*Marinobacter*, *Oceanicaulis*, *Algoriphagus*, and *Muricauda*) that responded positively to *P. tricornutum* exudates (Kim *et al.*, 2021). These same genera responded positively to algal spent medium in our study, indicating that spent media can generate similar effects to 'live' algal exudates. Along with exudate composition, this could also be due to pH, which is higher in both the algae present and spent media conditions, relative to the fresh media control. However, the communities with spent medium still differed from those with algae present: they were less diverse and some individual ASVs had divergent responses to the treatments. Several important factors may contribute to these differences. First, introduction of a bacterial community has been shown to affect algal gene expression in comparison to axenic controls, indicating that algae are actively responding to the microbial community (Shibl *et al.*, 2020). Other factors arising from algal presence, such as exchange of gases and volatiles (Zuo, 2019), the phycosphere microenvironment around algal cells (Seymour *et al.*, 2017), and temporal dynamics (Uchimiya

acid (Figs 6b, S7, S12). The magnitudes of the strongest responses to lumichrome were less than those observed with 4-hydroxybenzoic acid. The maximum log fold change observed for lumichrome was 0.83, in comparison with 2.4 for 4-hydroxybenzoic acid. No ASVs consistently increased with lumichrome addition across algal treatments, while two (*Thalassospira* ASV7 and *Seohaeicola* ASV10) decreased in relative abundance with lumichrome addition under all three algal conditions. *Alcanivorax* ASV14 responded negatively to lumichrome in the algae-free condition, and the isolate match *Alcanivorax* EA2 also had repressed growth in response to riboflavin (of which lumichrome is a degradation product) addition (Fig. 5).

To better assess potential indirect effects of metabolite additions, we investigated the impacts of exogenous additions of 4-hydroxybenzoic acid and lumichrome on axenic algal growth

et al., 2021) likely also contribute to these differences. Indeed, previous work involving the same enrichment cultures used here has shown that attachment can affect both algal carbon fixation and bacterial uptake of algal carbon (Samo *et al.*, 2018). Thus, the composition of algal exometabolites experienced by bacteria growing with algae likely differs from that of spent medium from axenic algae.

Comparing exometabolome compositions over time revealed variation in accumulation patterns of different metabolites over algal growth, which may indicate another factor influencing bacterial populations. Algal-associated microbial communities have been shown to vary with algal growth, for instance across different stages of an algal bloom (Zhou *et al.*, 2019). Previous work investigating algal–bacterial interactions across the diel cycle also found changes in endometabolome composition and transcriptomes from 1-day cycle to the next (Uchimiya *et al.*, 2021), indicating the importance of the longer time scales that we address here. Both the endometabolome and exometabolome of the marine cyanobacterium *Synechococcus elongatus* also vary over days (Fiore *et al.*, 2015). The extent of organic nitrogen transfer from *P. tricornutum* to bacteria has been shown to vary between bacterial taxa (Mayali *et al.*, 2022), and thus temporal changes in exudation of nitrogen-containing metabolites, which include the majority of metabolites identified here, suggest a possible mechanism for influencing bacterial functional guilds. Methodological limitations constrained our metabolite analysis, but despite only capturing a subset of metabolites, we still detected a number of novel diatom exometabolites that are produced throughout growth. We used SPE to recover metabolites and remove salts, and this approach, while commonly used, is known to have poor recovery of small, highly polar metabolites. Extraction efficiency of individual metabolites with these columns is influenced by metabolite size, aromaticity, and charge at pH 2, with smaller, non-aromatic, and charged metabolites having lower recovery (Johnson *et al.*, 2017). However, the PPL columns we used can recover *c.* 60% of dissolved organic matter from marine samples (Green *et al.*, 2014), so the metabolites detected likely contribute significantly to the dissolved organic carbon pool. The novel diatom exometabolites detected, and their enrichment in the exometabolome relative to the endometabolome, illustrate the importance of analyzing exudates, despite biases. For example, pyrrol-2-carboxylic acid was recently reported in the endometabolome of *P. tricornutum* and other diatoms and was found to increase in response to salt stress (Nikitashina *et al.*, 2022). We found that this metabolite, while detected in some cell pellet samples, was primarily an exometabolite. Additionally, the plant hormones salicylic acid, and indole-3-acetic acid, which we also identified as exometabolites, have the potential to impact algal physiology (Park *et al.*, 2013; Labeeuw *et al.*, 2016; Chung *et al.*, 2018) and can also act as bacterial substrates (Leveau & Gerards, 2008; Laird *et al.*, 2020). While more study of algal exometabolomes is needed to gain a mechanistic understanding of all exometabolites, here we demonstrate one approach to begin to ecologically classify exometabolites using both isolates and enrichment communities.

Our study shows that an individual substrate-class metabolite can predictably shift bacterial community composition in the context of either a complex exometabolome (algal spent medium), or in the presence of an algal host, although the magnitude of these shifts varied with condition. The organic acid 4-hydroxybenzoic acid is exuded by both *P. tricornutum* and *Synechococcus elongatus* (Fiore *et al.*, 2015), and has been shown to influence both bacterial and fungal community compositions in the rhizosphere (Zhou *et al.*, 2012), suggesting it is an important exometabolite in a range of environments. This metabolite has been shown to be a plant autotoxin (Zhou *et al.*, 2012), but our results on axenic *P. tricornutum* did not show detectable inhibition of growth with its addition. Of the three isolates that were able to grow with 4-hydroxybenzoic acid as the primary carbon source, two (*Thalassospira 13M1* and *Roseibium 13C*) had corresponding ASVs which generally responded positively to both its addition and to algal spent medium, while the third (*Alcanivorax EA2*) did not. Together, this shows that growth in isolation is informative but not sufficient to predict competitive advantage. Our previous work provides a possible predictive metric based on substrate-class specialization, as it classified *Thalassospira 13M1* and *Roseibium 13C* as specializing in small carbon substrate utilization and *Alcanivorax EA2* as a macromolecule user, based on algal exudate incorporation (Mayali *et al.*, 2022). Furthermore, another isolate, *Devosia EAB7W2*, did not grow on 4-hydroxybenzoic acid, but the matching ASV showed a strong positive response to addition, suggesting this bacterium may require bacterial interactions or other substrates to gain an advantage from this exometabolite. Genome content provided a putative indicator for selective advantage in this case: the three responsive genera in the community (*Thalassospira*, *Roseibium* (*Labrenzia*), and *Devosia*) were the only three of our bacterial isolates with matched ASV's whose genomes contained the *pobA* gene, whose product converts 4-hydroxybenzoate to protocatechuate, an important entry to the TCA cycle (Harwood & Parales, 1996). Notably, *Alcanivorax EA2* lacks the *pobA* gene, so while it can utilize 4-hydroxybenzoic acid when grown by itself, it may not be able to compete as effectively for it. Our results thus suggest that both metabolite composition (presence of preferred substrates) and the community (e.g. bacterial interactions) are important for predicting positive response to a particular metabolite.

While 4-hydroxybenzoic acid exemplifies selective growth promotion as a potential mechanism of algal impacts on microbial communities, inhibition effects, while not as straightforward, are also an important factor in modulating microbial communities. A small number of ASVs responded positively to algal spent media and negatively to algal presence (*Thalassospira* and *Roseibium* (*Labrenzia*) and *Marinobacter*). This suggests that other factors associated specifically with algal presence selectively reduce the growth of these taxa, and that excess levels of an algal exometabolite to which they are specialized (i.e. 4-hydroxybenzoic acid for *Thalassospira* and *Roseibium* (*Labrenzia*)) can overcome this inhibition. Interestingly, all three taxa are from the same functional guild, classified as specializing in small carbon compounds from algal exudates (Mayali *et al.*, 2022). Competition with algae

for inorganic nutrients may contribute to this effect. A previous study using porous microplates with gradients of inorganic nutrients and algal DOC found that growth of *Marinobacter* 3–2 (the same isolate used here) was dependent on access to inorganic nutrients along with algal DOC (Kim *et al.*, 2021). *P. tricornutum* also produces antimicrobial fatty acids (Desbois *et al.*, 2009), suggesting another potential mechanism of selective controls of bacterial growth.

While lumichrome was selected partially as another control (because it is not classified as a substrate exometabolite), the effects of its addition highlight interactions that may involve other factors such as signaling or facilitating chemical reactions. Lumichrome, a vitamin derivative, did have significant effects on individual ASV relative abundances (Fig. 6). Although we did not detect a statistically significant effect of lumichrome on final *P. tricornutum* chlorophyll *a* fluorescence (*P*-value = 0.06), there was a trend toward increased fluorescence with lumichrome addition, and lumichrome has previously been shown to stimulate the growth of *P. tricornutum* and of other microalgae in different experiments (Lopez *et al.*, 2019; Brisson *et al.*, 2021), and to change the endometabolite composition of *Chlorella sorokiniana* (Lopez *et al.*, 2019). This suggests that differences in microbial abundances occurring when algae are present may be indirect effects due to lumichrome altering algal physiology which in turn affects the bacteria. Conversely, lumichrome is a degradation product of riboflavin (vitamin B2) and can also act as a bacterial quorum-sensing mimic (Rajamani *et al.*, 2008), so it may have a more direct effect on bacterial community members.

Our results demonstrate the multifaceted role of algal extracellular metabolites in shaping algal-associated bacterial communities. We found that algal exudates can influence community composition, identified a suite of novel *P. tricornutum* exometabolites, and further characterized one exometabolite, 4-hydroxybenzoic acid. We found only some bacterial isolates could use 4-hydroxybenzoic acid as a carbon source, and addition of it positively selected for those taxa in complex communities, demonstrating that a selective bacterial growth substrate represents one mechanism by which algal exudates can modulate the microbial community. Our work also provides evidence for the presence of additional controls requiring algal presence that selectively keep taxa specializing in algal carbon exometabolite consumption in check relative to taxa with other ecological strategies. Furthermore, our temporal analysis illustrates how the algal exometabolome has the potential to modulate bacterial ecophysiology as a function of algal growth, hinting at many other exometabolites yet to be characterized that could positively or negatively influence specific bacterial groups. This work advances our understanding of the algal exometabolome and its importance in algal–bacterial interactions and microbial community composition.

Acknowledgements

Competing interests

None declared.

Author contributions

VB, MT, TRN and RKS developed the concept and experimental plan. VB conducted the experiments and analyzed the data. CS conducted DNA extraction and processing. JK analyzed bacterial isolate genomes for genes related to 4-hydroxybenzoic acid and shikimate degradation. XM and TS provided expertise on the bacterial isolates and enrichment cultures. VB and SMK conducted the metabolomic analysis. All authors contributed to writing and editing the manuscript.

ORCID

Vanessa Brisson https://orcid.org/0000-0003-1398-1664
Jeffrey Kimbrel https://orcid.org/0000-0001-7213-9392
Suzanne M. Kosina https://orcid.org/0000-0003-2885-1248
Xavier Mayali https://orcid.org/0000-0002-2170-0773
Trent R. Northen https://orcid.org/0000-0001-8404-3259
Ty Samo https://orcid.org/0000-0002-0548-4599
Rhona K. Stuart https://orcid.org/0000-0001-5916-9693
Michael Thelen https://orcid.org/0000-0002-2479-5480

Data availability

Sequencing data are deposited in the NCBI Sequence Read Archive under BioProject no. PRJNA803592. Metabolomics LC–MS/MS raw data and metadata are deposited in the NIH Common Fund's National Metabolomics Data Repository (supported by NIH grant U2C-DK119886) website, the Metabolomics Workbench, https://www.metabolomicsworkbench.org under Project ID PR001317 and Study ID ST002077, and can be accessed directly via the Project doi: 10.21228/M8GH6P. Analysis scripts are available on GitHub (https://github.com/vbrisson/Algal_Exometabolites_Shape_Bacterial_Communities).

References

Aitchison J. 1982. The statistical-analysis of compositional data. *Journal of the Royal Statistical Society. Series B: Methodological* 44: 139–177.

Apprill A, McNally S, Parsons R, Weber L. 2015. Minor revision to V4 region SSU rRNA 806R gene primer greatly increases detection of SAR11 bacterioplankton. *Aquatic Microbial Ecology* 75: 129–137.

Astacio LMD, Prabhakara KH, Li ZQ, Mickalide H, Kuehn S. 2021. Closed microbial communities self-organize to persistently cycle carbon. *Proceedings of the National Academy of Sciences, USA* 118: 9.

Becker JW, Berube PM, Follett CL, Waterbury JB, Chisholm SW, DeLong EF, Repeta DJ. 2014. Closely related phytoplankton species produce similar suites of dissolved organic matter. *Frontiers in Microbiology* 5: 14.

New
Phytologist

Berges JA, Franklin DJ, Harrison PJ. 2001. Evolution of an artificial seawater medium: improvements in enriched seawater, artificial water over the last two decades. *Journal of Phycology* **37**: 1138–1145.

Bowen BP, Northen TR. 2010. Dealing with the unknown: metabolomics and metabolite atlases. *Journal of the American Society for Mass Spectrometry* **21**: 1471–1476.

Brisson V, Mayali X, Bowen B, Golini A, Thelen M, Stuart RK, Northen TR. 2021. Identification of effector metabolites using exometabolite profiling of diverse microalgae. *mSystems* **6**: e0083521.

Callahan BJ, McMurdie PJ, Rosen MJ, Han AW, Johnson AJA, Holmes SP. 2016. DADA2: high-resolution sample inference from Illumina amplicon data. *Nature Methods* **13**: 581.

Chisti Y. 2007. Biodiesel from microalgae. *Biotechnology Advances* **25**: 294–306.

Chorazyczewski AM, Huang IS, Abdulla H, Mayali X, Zimba PV. 2021. The influence of bacteria on the growth, lipid production, and extracellular metabolite accumulation by *Phaeodactylum tricornutum* (Bacillariophyceae). *Journal of Phycology* **57**: 931–940.

Chung TY, Kuo CY, Lin WJ, Wang WL, Chou JY. 2018. Indole-3-acetic-acid-induced phenotypic plasticity in Desmodesmus algae. *Scientific Reports* **8**: 13.

Deng Y, Mauri M, Vallet M, Staudinger M, Allen RJ, Pohnert G. 2022. Dynamic diatom-bacteria consortia in synthetic plankton communities. *Applied and Environmental Microbiology* **88**: 16.

Desbois AP, Mearns-Spragg A, Smith VJ. 2009. A fatty acid from the diatom *Phaeodactylum tricornutum* is antibacterial against diverse bacteria including multi-resistant *Staphylococcus aureus* (MRSA). *Marine Biotechnology* **11**: 45–52.

Falkowski P. 2012. Ocean science: the power of plankton. *Nature* **483**: S17–S20.

Ferrer-Gonzalez FX, Widner B, Holderman NR, Glushka J, Edison AS, Kujawinski EB, Moran MA. 2021. Resource partitioning of phytoplankton metabolites that support bacterial heterotrophy. *ISME Journal* **15**: 762–773.

Fiore C, Longnecker K, Soule M, Kujawinski E. 2015. Release of ecologically relevant metabolites by the cyanobacterium *Synechococcus elongatus* CCMP 1631. *Environmental Microbiology* **17**: 3949–3963.

Fu H, Uchimiya M, Gore J, Moran MA. 2020. Ecological drivers of bacterial community assembly in synthetic phycospheres. *Proceedings of the National Academy of Sciences, USA* **117**: 3656–3662.

Gloor GB, Macklaim JM, Pawlowsky-Glahn V, Egozcue JJ. 2017. Microbiome datasets are compositional: and this is not optional. *Frontiers in Microbiology* **8**: 6.

Green NW, Perdue EM, Aiken GR, Butler KD, Chen HM, Dittmar T, Niggemann J, Stubbins A. 2014. An intercomparison of three methods for the large-scale isolation of oceanic dissolved organic matter. *Marine Chemistry* **161**: 14–19.

Guillard RR, Ryther JH. 1962. Studies of marine planktonic diatoms. 1. Cyclotella nana Hustedt, and Detonula confervacea (Cleve) Gran. *Canadian Journal of Microbiology* **8**: 229–239.

Harrison PJ, Waters RE, Taylor FJR. 1980. A broad-spectrum artificial seawater medium for costal and open ocean phytoplankton. *Journal of Phycology* **16**: 28–35.

Harwood CS, Parales RE. 1996. The beta-ketoadipate pathway and the biology of self-identity. *Annual Review of Microbiology* **50**: 553–590.

Hu CH, Zhao SX, Li KR, Yu H. 2019. Microbial degradation of nicotinamide by a strain *Alcaligenes* sp. P156. *Scientific Reports* **9**: 3647.

Johnson WM, Soule MCK, Kujawinski EB. 2017. Extraction efficiency and quantification of dissolved metabolites in targeted marine metabolomics. *Limnology and Oceanography-Methods* **15**: 417–428.

Kieft B, Li Z, Bryson S, Hettich RL, Pan CL, Mayali X, Mueller RS. 2021. Phytoplankton exudates and lysates support distinct microbial consortia with specialized metabolic and ecophysiological traits. *Proceedings of the National Academy of Sciences, USA* **118**: 12.

Kim H, Kimbrel JA, Vaiana CA, Wollard JR, Mayali X, Buie CR. 2021. Bacterial response to spatial gradients of algal-derived nutrients in a porous microplate. *ISME Journal* **10**: 1036–1045.

Kimbrel JA, Samo TJ, Ward C, Nilson D, Thelen MP, Siccardi A, Zimba P, Lane TW, Mayali X. 2019. Host selection and stochastic effects influence bacterial community assembly on the microalgal phycosphere. *Algal Research-Biomass Biofuels and Bioproducts* **40**: 10.

Labeeuw L, Khey J, Bramucci AR, Atwal H, de la Mata AP, Harynuk J, Case RJ. 2016. Indole-3-acetic acid is produced by *Emiliania huxleyi* coccolith-bearing cells and triggers a physiological response in bald cells. *Frontiers in Microbiology* **7**: 16.

Laird TS, Flores N, Leveau JHJ. 2020. Bacterial catabolism of indole-3-acetic acid. *Applied Microbiology and Biotechnology* **104**: 9535–9550.

Leveau JHJ, Gerards S. 2008. Discovery of a bacterial gene cluster for catabolism of the plant hormone indole 3-acetic acid. *FEMS Microbiology Ecology* **65**: 238–250.

Lin H, Das Peddada S. 2020. Analysis of compositions of microbiomes with bias correction. *Nature Communications* **11**: 11.

Lopez BR, Palacios OA, Bashan Y, Hernandez-Sandoval FE, de Bashan LE. 2019. Riboflavin and lumichrome exuded by the bacterium *Azospirillum brasilense* promote growth and changes in metabolites in *Chlorella sorokiniana* under autotrophic conditions. *Algal Research-Biomass Biofuels and Bioproducts* **44**: 101696.

Mata TM, Martins AA, Caetano NS. 2010. Microalgae for biodiesel production and other applications: A review. *Renewable & Sustainable Energy Reviews* **14**: 217–232.

Mayali X, Samo T, Kimbrel J, Stuart RK, Morris M, Rolison K, Ramon C, Kim Y-M, Munoz-Munoz N, Nicora C et al. 2022. Single cell carbon and nitrogen incorporation and remineralization profiles are uncoupled from phylogenetic groupings of diatom-associated bacteria. *bioRxiv.* doi: 10.1101/2022.07.01.498368.

McMurdie PJ, Holmes S. 2013. PHYLOSEQ: an R package for reproducible interactive analysis and graphics of microbiome census data. *PLoS ONE* **8**: 11.

Moran MA, Kujawinski EB, Schroer WF, Amin SA, Bates NR, Bertrand EM, Braakman R, Brown CT, Covert MW, Doney SC et al. 2022. Microbial metabolites in the marine carbon cycle. *Nature Microbiology* **7**: 508–523.

Nikitashina V, Stettin D, Pohnert G. 2022. Metabolic adaptation of diatoms to hypersalinity. *Phytochemistry* **201**: 13.

Orellana LH, Ben Francis T, Ferraro M, Hehemann JH, Fuchs BM, Amann RI. 2022. Verrucomicrobiota are specialist consumers of sulfated methyl pentoses during diatom blooms. *ISME Journal* **16**: 630–641.

Parada AE, Needham DM, Fuhrman JA. 2016. Every base matters: assessing small subunit rRNA primers for marine microbiomes with mock communities, time series and global field samples. *Environmental Microbiology* **18**: 1403–1414.

Park WK, Yoo G, Moon M, Kim C, Choi YE, Yang JW. 2013. Phytohormone supplementation significantly increases growth of *Chlamydomonas reinhardtii* cultivated for biodiesel production. *Applied Biochemistry and Biotechnology* **171**: 1128–1142.

Prabhakara KH, Kuehn S. 2022. Algae drive convergent bacterial community assembly when nutrients are scarce. *bioRxiv.* doi: 10.1101/2022.06.27.497809.

Rajamani S, Bauer WD, Robinson JB, Farrow JM, Pesci EC, Teplitski M, Gao MS, Sayre RT, Phillips DA. 2008. The vitamin riboflavin and its derivative lumichrome activate the LasR bacterial quorum-sensing receptor. *Molecular Plant–Microbe Interactions* **21**: 1184–1192.

Samo TJ, Kimbrel JA, Nilson DJ, Pett-Ridge J, Weber PK, Mayali X. 2018. Attachment between heterotrophic bacteria and microalgae influences symbiotic microscale interactions. *Environmental Microbiology* **20**: 4385–4400.

Seyedsayamdost MR, Wang RR, Kolter R, Clardy J. 2014. Hybrid biosynthesis of roseobacticides from algal and bacterial precursor molecules. *Journal of the American Chemical Society* **136**: 15150–15153.

Seymour JR, Amin SA, Raina JB, Stocker R. 2017. Zooming in on the phycosphere: the ecological interface for phytoplankton–bacteria relationships. *Nature Microbiology* **2**: 12.

Shibl AA, Isaac A, Ochsenkuhn MA, Cardenas A, Fei C, Behringer G, Arnoux M, Drou N, Santos MP, Gunsalus KC et al. 2020. Diatom modulation of select bacteria through use of two unique secondary metabolites. *Proceedings of the National Academy of Sciences, USA* **117**: 27445–27455.

Swift CL, Louie KB, Bowen BP, Olson HM, Purvine SO, Salamov A, Mondo SJ, Solomon KV, Wright AT, Northen TR et al. 2021. Anaerobic gut fungi are an untapped reservoir of natural products. *Proceedings of the National Academy of Sciences, USA* **118**: e2019855118.

Teeling H, Fuchs BM, Becher D, Klockow C, Gardebrecht A, Bennke CM, Kassabgy M, Huang SX, Mann AJ, Waldmann J et al. 2012. Substrate-

controlled succession of marine bacterioplankton populations induced by a phytoplankton bloom. *Science* **336**: 608–611.

Thornton DCO. 2014. Dissolved organic matter (DOM) release by phytoplankton in the contemporary and future ocean. *European Journal of Phycology* **49**: 20–46.

Uchimiya M, Schroer W, Olofsson M, Edison AS, Moran MA. 2021. Diel investments in metabolite production and consumption in a model microbial system. *ISME Journal* **16**: 1306–1317.

Yao YS, Sun T, Wang T, Ruebel O, Northen T, Bowen BP. 2015. Analysis of metabolomics datasets with high-performance computing and metabolite atlases. *Metabolites* **5**: 431–442.

Zhalnina K, Louie KB, Hao Z, Mansoori N, da Rocha UN, Shi SJ, Cho HJ, Karaoz U, Loque D, Bowen BP *et al.* 2018. Dynamic root exudate chemistry and microbial substrate preferences drive patterns in rhizosphere microbial community assembly. *Nature Microbiology* **3**: 470–480.

Zhou J, Chen GF, Ying KZ, Jin H, Song JT, Cai ZH. 2019. Phycosphere microbial succession patterns and assembly mechanisms in a marine dinoflagellate bloom. *Applied and Environmental Microbiology* **85**: 17.

Zhou XG, Yu GB, Wu FZ. 2012. Responses of soil microbial communities in the rhizosphere of cucumber (*Cucumis sativus* L.) to exogenously applied *p*-hydroxybenzoic acid. *Journal of Chemical Ecology* **38**: 975–983.

Zuo ZJ. 2019. Why algae release volatile organic compounds – the emission and roles. *Frontiers in Microbiology* **10**: 7.

Supporting Information

Additional Supporting Information may be found online in the Supporting Information section at the end of the article.

Fig. S1 Schematic of experiments conducted for this study.

Fig. S2 Phosphate and nitrate depletion from Enriched Saltwater Artificial Water medium by axenic *Phaeodactylum tricornutum*.

Fig. S3 Media pH.

Fig. S4 Analysis of the impacts of prevalence cut-off on amplicon sequence variant retention.

Fig. S5 Algal (*Phaeodactylum ricornutum*) growth and sampling for metabolomics analysis.

Fig. S6 Maximum likelihood phylogenetic tree of amplicon sequence variant sequences.

Fig. S7 Relative abundances of amplicon sequence variants in individual samples (15 flasks × 3 time points), grouped by conditions and time points.

Fig. S8 Microbial community alpha diversity as measured by Shannon diversity index.

Fig. S9 Ternary plot showing bacterial amplicon sequence variants responses to algal (*Phaeodactylum ricornutum*) exudates and algal presence.

Fig. S10 Bacterial isolate growth results for the two metabolites that supported significant growth and for the no-metabolite added controls for comparison.

Fig. S11 Responses of individual amplicon sequence variants to exogenous addition of 4-hydroxybenzoic acid (all time points).

Fig. S12 Responses of individual amplicon sequence variants to exogenous addition of lumichrome (all time points).

Fig. S13 Impacts of exogenous metabolite additions on axenic *Phaeodactylum tricornutum* growth.

Methods S1 Growth medium composition.

Methods S2 DNA extraction.

Methods S3 Amplicon sequence processing.

Methods S4 Statistical analyses.

Table S1 Liquid chromatography–tandem mass spectrometry instrument and parameters for metabolomics analysis.

Table S2 Permutational analysis of variance of prokaryotic community composition based on relative abundances of 62 amplicon sequence variants.

Table S3 ANOVA of microbial community alpha diversity as measured by the Shannon diversity index.

Table S4 Metabolite identifications.

Table S5 Metabolite relative intensities.

Table S6 Genes involved in 4-hydroxybenzoic acid and shikimic acid degradation, and corresponding search terms used in genomic analysis.

Table S7 Summary of responses of bacterial isolates and congeneric amplicon sequence variants.

Table S8 Permutational analysis of variance of prokaryotic community composition based on relative abundances of 62 amplicon sequence variants.

Please note: Wiley is not responsible for the content or functionality of any Supporting Information supplied by the authors. Any queries (other than missing material) should be directed to the *New Phytologist* Central Office.